Troponin I Inhibitory Peptide (96−115) Has an Extended Conformation When Bound to Skeletal Muscle Troponin C†

Griselda Hernández,*,‡ Donald K. Blumenthal,§ Michael A. Kennedy,|| Clifford J. Unkefer,‡ and Jill Trewhella*,‡

Chemical Science and Technology Division, Mail Stop G758, Los Alamos National Laboratory, Los Alamos, New Mexico 87545, Department of Pharmacology & Toxicology, University of Utah, Salt Lake City, Utah 84112, and Macromolecular Structure and Dynamics, Environmental Molecular Sciences Laboratory, Pacific Northwest National Laboratory, Richland, Washington 99352

Received January 21, 1999; Revised Manuscript Received April 7, 1999

ABSTRACT: We have utilized CD and NMR spectroscopy to study the conformation of the troponin I (TnI) inhibitory peptide [TnI(96−115)] free in solution and when bound to troponin C (TnC). Analysis of the CD spectrum of the free peptide in aqueous solution indicates it is only ∼3% helix. Upon complex formation with TnC, there is no change in total helix content compared to the sum of the free components. The NMR data support a predominantly extended conformation for the free peptide. TnI(96−115) bound to TnC was selectively observed by NMR using deuterated TnC (dTnC). For the 1:1 ratio of TnI(96−115) to dTnC used, 95% of the peptide was bound to dTnC. The chemical shifts of the TnC-bound peptide resonances are similar to those of the free peptide, indicating that the change in peptide conformation as a consequence of binding to TnC is small. For the TnC-bound TnI(96−115) peptide, the ratios of sequential $H^{\alpha}-H^{N}$ to intraresidue $H^{N}-H^{\alpha}$ NOE cross-peak volumes support a predominantly extended conformation, possibly kinked at Gly^{104}. The results presented here are in agreement with sequence analysis predictions for TnI(96−115) as a free peptide or within the intact TnI sequence. The predominantly extended structure for the 96−115 inhibitory sequence segment of TnI with a kink at Gly^{104} may facilitate its binding alternately to actin or TnC in response to the Ca^{2+} signals that control thick and thin filament interactions during the contractile cycle.

The troponin complex functions as a calcium-dependent switch in muscle contraction (reviewed in ref *1*), regulating the interactions between the interdigitated thick and thin filaments that are proposed to slide past each other during the contractile cycle. Troponin has three components: troponin C (TnC)[1] which binds Ca^{2+}, troponin I (TnI) which inhibits the interactions between the thick and thin filaments in the absence of the Ca^{2+} signal, and troponin T (TnT) which anchors troponin to the thin filament and is believed to be involved in the transmission of regulatory signals along the thin filament. The crystal structure of TnC exhibits two globular domains separated by an extended α-helix of seven to eight turns (*2*, *3*). The high-affinity C-terminal Ca^{2+}-binding sites of TnC are always occupied under physiological conditions, while the lower-affinity N-terminal Ca^{2+}-binding sites are the regulatory sites (*4*). Contraction is initiated when Ca^{2+} binds to the regulatory sites, inducing a conformational change that results in the exposure of hydrophobic residues in a cleft within the N-terminal domain (*5*, *6*). This conformational change signals TnI to release its inhibition of the interaction between the myosin headgroups of the thick filaments and the actin molecules of the thin filaments, thus switching on the actomyosin ATPase activity that drives muscle contraction.

We have been studying the interactions of skeletal muscle TnC and TnI in order to shed light on the molecular basis for this switch mechanism. Neutron contrast variation studies of the Ca^{2+} saturated complex of intact TnI with deuterated TnC (skeletal muscle forms) support a model for a fully extended dumbbell-shaped TnC with an even more extended TnI forming a superhelical spiral structure that encompasses TnC and passes through or near the hydrophobic clefts on each globular domain (*7*, *8*). The dimensions of the superhelical spiral are consistent with its having a predominantly α-helical secondary structure. On the basis of the TnC−TnI structure derived from the neutron scattering experiments, we proposed a structural mechanism for the "switch" function of TnC which involves the binding and release of TnI by TnC via an opening and closing of the hydrophobic cleft in the N-terminal domain of TnC. Recently, Mendelson and

† This work was performed under the auspices of the Department of Energy (Contract W-7405-ENG-36) and supported in part by NIH Grant GM40528 (J.T.) and by the National Stable Isotope Resource NIH/National Center for Resources (RR 02231). Peptide synthesis, amino acid, and mass spectroscopy analyses were carried out at the University of Utah facilities that are supported in part by NCI Grant 5 P30 CA42014. Preliminary NMR data were acquired using facilities at the Environmental Molecular Science Laboratory, Pacific Northwest National Laboratory.

* Corresponding authors. J.T.: jtrewhella@lanl.gov or (505) 667-2031. G.H.: griselda@lanl.gov or (505) 665-6796.

‡ Los Alamos National Laboratory.

§ University of Utah.

|| Pacific Northwest National Laboratory.

[1] Abbreviations: DQF-COSY, double-quantum-filtered correlated spectroscopy; FMOC, 9-fluorenylmethyloxycarbonyl; NOE, nuclear Overhauser effect; TFE, 2,2,2-trifluoroethanol; TnC, troponin C; TnI, troponin I; dTnC, deuterated troponin C; hTnC, protiated troponin C; Pmc-Arg, *Nγ*-2,2,5,7,8-pentamethylchroman-6-sulfonyl-L-arginine; TR-NOE, transferred nuclear Overhauser effect.

10.1021/bi990150q CCC: $18.00
Published on Web 05/07/1999

co-workers (*9*) have published the results of a neutron contrast variation study in which the structures of deuterated forms of TnC and TnI were evaluated while in the ternary troponin complex which also includes TnT. Their results agree with our studies of the binary complex with respect to the extended TnC structure. However, they find a less extended structure for TnI than is observed in the binary complex, possibly due to additional interactions between TnI and TnT.

The relatively low solubilities and high molecular weights of the binary or ternary complexes of troponin components are such that they have proven to be resistant to high-resolution structural analysis using crystallography or NMR. The neutron experiments therefore provide us the only direct structural data for the interactions between the intact proteins. While they provide a framework for testing ideas about troponin regulation, significant questions about the high-resolution structures and interactions of the components remain. Many groups have turned to studies of functionally relevant fragments of TnC and TnI to piece together higher-resolution information. Recently, a crystal structure of skeletal TnC complexed with TnI(1−47) has been determined (*10*). The N-terminal sequence of TnI has been implicated in the regulation of the inhibitory function (*11*). The crystal structure shows that the two globular domains of TnC are closer to each other than in the crystal structure of TnC, and 31 residues of the TnI(1−47) form an α-helix that interacts strongly with the hydrophobic cleft in the C-terminal domain of TnC. This interaction with the N-terminal sequence of TnI and the compaction of TnC are not consistent with the current neutron scattering-derived model for the intact TnC−TnI complex (*8*). Solution scattering studies (*12*) previously have shown that TnC binding peptides (e.g., mellitin) can induce a conformational collapse of TnC. In the case of mellitin, the observed collapse is very similar to that seen for calmodulin when it binds to amphipathic, helical peptides (*13*). However, the solution scattering experiments failed to detect evidence for TnC undergoing a compaction upon binding TnI(96−115), TnI-(1−40), or TnI(1−30).

The evaluation of structural and mechanistic models for the TnC−TnI interaction clearly requires additional high-resolution structural data for TnI within the complex. We report here studies of the avian skeletal muscle TnI inhibitory peptide, corresponding to residues 96−115, complexed with TnC. The TnI(96−115) peptide contains the minimum sequence (residues 104−115) required to fully inhibit actomyosin ATPase activity (*14*) and hence has been widely used in biophysical studies of TnC−TnI interactions. Campbell and Sykes (*15*) used transferred NOE (TRNOE) measurements to study the TnI(104−115) peptide bound to TnC. We chose to study the longer peptide sequence TnI(96−115) because it provides additional interactions for stabilizing the bound peptide conformation and binds to TnC with a 17-fold higher affinity [$K_d = 0.47$ μM (*16*)]. For the NMR studies, the TnC was deuterated to facilitate observation of the bound TnI peptide proton resonances, similar to the approach used for the calmodulin−melittin system (*17*). Deuteration of TnC allows the acquisition of NOESY spectra of TnI(96−115) under conditions for which approximately 95% of the peptide fragments are bound to TnC. Thus, both cross-peak intensity distortions (*18*) and the appearance of spurious cross-peaks due to spin diffusion between the peptide and the protein that have been observed in TRNOE measurements (*19*, *20*) are circumvented.

MATERIALS AND METHODS

Protein and Peptide Preparation. Avian skeletal muscle TnC was prepared in both protiated (hTnC) and perdeuterated (dTnC) forms using bacterial expression systems as previously described (*7*). TnI(96−115) peptide was synthesized as Ac-SQKLFDLRGKFKRPPLRRVR-amide. Ac denotes an acetylated N-terminus. Peptides were synthesized on an Applied Biosystems 431 peptide synthesizer using standard FMOC chemistry. The peptide was synthesized on an amide resin using *N*-methylpyrrolidinone as the solvent. Pmc-Arg and trityl-Gln were used for side chain protection. The synthesis and cleavage were performed by the University of Utah Huntsman Cancer Center DNA/Peptide Synthesis Facility. The cleaved peptide was purified with a semi-preparative Vydac C4 HPLC column using a water/acetonitrile gradient with 0.1% trifluoroacetic acid. The peptide was analyzed by amino acid analysis and ion electrospray mass spectrometry to confirm its composition and mass.

CD Spectroscopy. Protein and peptide were dissolved in 50 mM KCl, 0.1 mM $CaCl_2$, 0.1 mM sodium azide, and 0.02 mM dithiothreitol, and the pH was adjusted to 5.9 by addition of diluted KOH or HCl. Samples of $4Ca^{2+}$·dTnC·TnI(96−115) complex, free TnC, and free TnI(96−115) were measured in a 10 mm path length cell with 2.5 or 10 μM peptide in aqueous buffer or mixtures of buffer and trifluoroethanol (TFE), respectively. CD spectra were recorded at room temperature using a Jasco 720 spectropolarimeter calibrated using ammonium d_{10}-camphorsulfonic acid as described by the instrument manufacturer. Spectra were obtained using a 2.0 nm spectral bandwidth, a 2.0 s response time, and either a 20 or 50 nm/min scan rate. The spectra represent the average of five accumulated scans (for the 50 nm/min scan rate) or three accumulated scans (for the 20 nm/min scan rate). The helical content of the peptide was calculated by using the empirical equation (*21*)

$$f_H = [\Theta]_{222}/\{[\Theta]^{\infty}_{H}[1 - (k/n)]\} \quad (1)$$

where $[\Theta]^{\infty}_{H}$ is the mean molar residue ellipticity of an infinite helix (−37400°), k is the chain length dependence factor (2.5), and n is the number of residues in a typical α-helical segment (9). The mean molar residue ellipticity at 222 nm, $[\Theta]_{222}$, was calculated using the equation

$$[\Theta]_{222} = \Theta M_r/100LC \quad (2)$$

where Θ is in degrees, L is the cell path length (decimeters), C is the peptide concentration (grams per milliliter), and M_r is the mean residue molecular weight (110).

NMR Spectroscopy. Sample buffers contained 50 mM KCl, 0.1 mM sodium azide, and 1 mM d_{10}-dithiothreitol in 90% H_2O/10% D_2O. The dTnC was exhaustively dialyzed against the NMR buffer supplemented with 30 μM $CaCl_2$ and 10 mM sodium acetate at pH 6.0. This calcium concentration is sufficient for essentially complete loading of 4 equiv of calcium per mole of TnC (*4*). Calcium saturation of the dTnC was confirmed by the H^N chemical shift values of the glycines in the calcium-binding loops: 10.78 ppm for Gly^{71}, 10.64 ppm for Gly^{35}, and 10.37 ppm for both Gly^{111} and

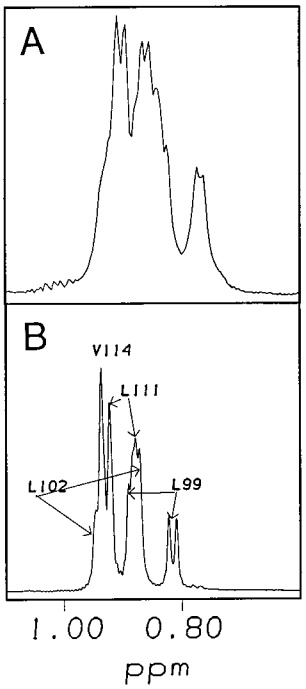

FIGURE 1: 500 MHz ^{1}H NMR spectra of the methyl region at 35 °C and pH 6.0 for (A) $4Ca^{2+}$·dTnC·TnI(96−115) and (B) free TnI(96−115).

Gly^{147}. Each of these resonances is within 0.05 ppm of the previously published results with calcium-saturated TnC (*22*). The large downfield migration of these resonances upon calcium binding provides an effective monitor of the calcium titration of TnC (*23*).

Titration of dTnC with TnI(96−115) was performed by adding aliquots of a 4.0 mM TnI(96−115) solution to dTnC, initially at 1.0 mM. Free TnI(96−115) spectra were acquired at pH 5.7 and at a concentration of 2.0 or 4.0 mM. $4Ca^{2+}$·dTnC·TnI(96−115) complex spectra were acquired at pH 6.0 and at a concentration of ∼0.8 mM. Peptide samples in trifluoroethanol (TFE) were prepared by adding TFE (10, 20, and 30% v/v) to these solutions.

^{1}H NMR spectra were acquired on a Bruker Advanced-500 spectrometer. Preliminary ^{1}H NMR spectra were collected on a Varian UNITY Plus-750 spectrometer. For spectra acquired at 35 °C, the water signal was suppressed using WATERGATE (*24*). The NOESY pulse sequence utilized flip-back pulses to avoid water saturation effects (*25*). Additional spectra were acquired for the free TnI(96−115), both in aqueous buffer and in the buffer/TFE mixtures, at 25, 15, and 5 °C to measure the temperature dependence of the chemical shift values.

NMR data were processed using the software FELIX 97.0 from BIOSYM/Molecular Simulations on a Silicon Graphics INDIGO 2 workstation.

RESULTS

Stoichiometric Binding of TnI(96−115) to TnC. Deuterated TnC was titrated with TnI(96−115). The use of dTnC allowed selective monitoring of the peptide methyl groups by NMR. Figure 1 shows the leucine (positions 99, 102, and 111) and valine (position 114) methyl group resonances of the TnC-bound peptide (Figure 1A) and free peptide (Figure 1B). Binding of the peptide to TnC results in an upfield

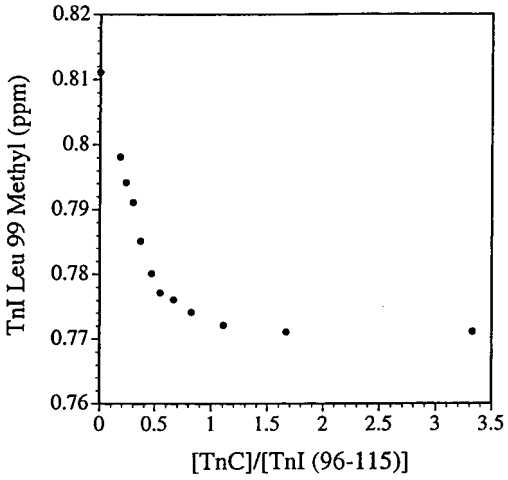

FIGURE 2: ^{1}H NMR chemical shift of the δCH_3 of the Leu^{99} resonance of TnI(96−115) as a function of the ratio of dTnC to peptide. The vertical axis is the observed chemical shift, referenced to water at 4.657 ppm, relative to 3-(trimethylethylsilyl)propionate, sodium salt (TSP), at pH 6.0 and 35 °C.

chemical shift and broadening of the methyl resonances. Figure 2 shows the chemical shift of a δCH_3 Leu^{99} TnI(96−115) proton resonance as a function of the molar ratio of [dTnC]/[TnI(96−115)]. The peptide is in fast exchange on the chemical shift time scale so that only one set of resonances is observed during the titration. The observed value is an average of the chemical shift of the free and bound states:

$$\delta_{obs} = p_f\delta_f + p_b\delta_b \quad (3)$$

where p_f and p_b are the free and bound fractions, respectively. δ_f and δ_b are the chemical shift values for the free and bound fractions, respectively, and δ_{obs} is the observed chemical shift. The insensitivity of the TnI(96−115) Leu^{99} methyl chemical shifts for [dTnC]/[TnI(96−115)] ratios above 1.0 is a clear indication that the peptide is fully bound. Using eq 3, the fraction of peptide bound to TnC calculated from the spectrum of the $4Ca^{2+}$·dTnC·TnI(96−115) complex (spectra shown below) was 95%. Therefore, cross-peak connectivities observed in the NOESY spectra of this complex reflect the conformation of the bound peptide. As a consequence, the ambiguities in the analysis of average NOE data derived from the free and bound peptide conformations in TRNOE experiments are circumvented.

CD Secondary Structure Analysis. The CD spectrum for the free peptide in aqueous solutions is typical of what is commonly assigned to random coil (Figure 3A). This result is consistent with the results obtained using AGADIR,[2] a secondary structure algorithm specific for peptides, which predicts ∼3% helical content. With increasing concentrations of the helix-stabilizing solvent TFE (*26*), the CD spectrum for the free peptide shows some helical character; ∼28% helix in 30% TFE and slightly higher (∼31%) in 50% TFE (Figure 3A). Therefore, the CD data show that the free TnI-(96−115) peptide has little or no α-helical character. Even in the presence of helix-inducing TFE, the disposition for forming α-helix is weak compared to that of α-helix-forming

[2] AGADIR, available on the World Wide Web at http://www.embl-heidelberg.de/Services/serrano/agadir-start.html.

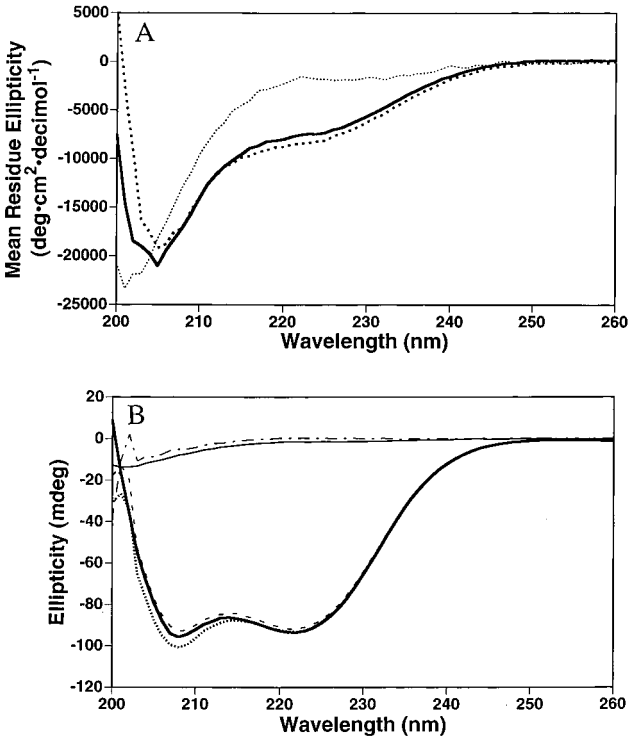

FIGURE 3: CD spectra measured at pH 5.9 for (A) free TnI(96−115) in aqueous solution (light dots), in 30% TFE (thick solid line), and in 50% TFE (heavy dots) and (B) free TnI(96−115) in aqueous solution (thin solid line), free TnC (thick solid line), and $4Ca^{2+}$·TnC·TnI(96−115) (dots). The difference spectra are for $4Ca^{2+}$·TnC·TnI(96−115) minus TnI(96−115) (dashed line) and $4Ca^{2+}$·TnC·TnI(96−115) minus TnC (dashed−dotted line).

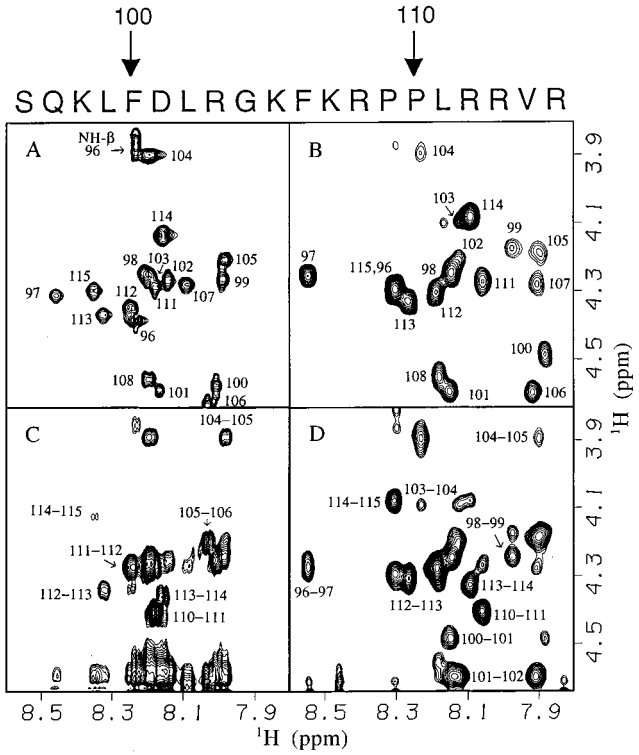

FIGURE 4: H^N-H^α region of the ^1H NMR spectra of free and TnC-bound TnI(96−115) at 35 °C: (A) TOCSY spectrum of free TnI(96−115), with a mixing time of 83 ms, at pH 5.7, (B) TOCSY spectrum of $4Ca^{2+}$·dTnC·TnI(96−115), with a mixing time of 23 ms, at pH 6.0, (C) NOESY spectrum of free TnI(96−115), with a mixing time of 300 ms, at pH 5.7, and (D) NOESY spectrum of $4Ca^{2+}$·dTnC·TnI(96−115), with a mixing time of 100 ms, at pH 6.0. For convenience, the inhibitory peptide sequence is given above the NMR spectra using the one-letter amino acid code with the indicated sequence numbering.

peptides such as mastoparan and melittin (*27*, *28*). The CD spectrum of the $4Ca^{2+}$·dTnC·TnI(96−115) complex is equivalent to the sum of the spectra of free TnC and TnI(96−115), all in aqueous solvent (Figure 3B). Difference spectra calculated by subtracting either the free TnC or the free TnI(96−115) spectrum from that of the complex exhibit no significant differences from the spectrum of the remaining component, i.e., free TnI(96−115) or TnC, respectively. These results indicate that there is no significant increase in helix content upon complex formation, and they are in stark contrast to the CD studies of the M13 peptide (corresponding to the calmodulin-binding domain of myosin light chain kinase) binding to calmodulin (*13*). The measured ellipticity of the calmodulin−M13 complex is much greater than the sum of the ellipticities of the individual components. Subsequent NMR studies (*29*) indicated that residues 3−21 of the M13 peptide, ∼80% of the entire peptide length, adopt an α-helical structure upon binding calmodulin.

NMR Secondary Structure Analysis of Free TnI(96−115). An increase in temperature will more readily break solute−solvent hydrogen bonds than intramolecular hydrogen bonds. If the temperature dependence of the chemical shift values ($\Delta\delta/\Delta T$) for backbone amide protons is linear and in the range of 0 to −3 ppb/K, intramolecular hydrogen bonds are generally inferred (*30*). For $\Delta\delta/\Delta T$ values between −6 to −10 ppb/K, the hydrogen-bonding interactions occur mainly between solute and solvent (*30*). The $\Delta\delta/\Delta T$ values for free TnI(96−115) in aqueous buffer are linear over the temperature range of 5−35 °C and vary from −6.0 to −12.3 ppb/K with an average value of −9.0 ppb/K. Thus, the temperature dependence of the chemical shift values for free TnI(96−115) indicates that the backbone amides in general do not participate in intramolecular hydrogen bonds. This result is in agreement with the CD data for the free peptide.

$^3J_{HN\alpha}$ spin−spin vicinal coupling constants expected for regular structures are ∼4 Hz for α- and 3_{10}-helices and 9−10 Hz for extended structures such as in β-sheets (*31*). Measured $^3J_{HN\alpha}$ coupling constants for the free TnI(96−115) peptide ranged between 8.0 and 9.8 Hz. In all cases, the resonance line widths are smaller than the observed coupling constants. Accounting for antiphase cancellation (*32*), the $^3J_{HN\alpha}$ coupling constants are at most 10% smaller than the observed values. Thus, the observed $^3J_{HN\alpha}$ spin−spin vicinal coupling constants for the free peptide indicate a mostly extended conformation for each of the residues.

Resonance assignments for free TnI(96−115) were obtained from DQF-COSY and TOCSY spectra following standard procedures (*31*). Sequential assignments were made using $H^\alpha-H^N$, H^N-H^N, and $H^\beta-H^N$ sequential connectivities in the NOESY spectra. Free TnI(96−115) resonance assignments are denoted in the TOCSY spectrum in Figure 4A. All H^N-H^α intraresidue cross-peaks for the free TnI(96−115) are observed with the obvious exception of prolines 109 and 110. The free TnI(96−115) NOESY spectrum is shown in Figure 4C where only the cross-peaks arising from sequential connectivities are labeled for clarity.

Helices exhibit nonsequential medium-range NOE connectivities arising from residues in the adjacent turns. In

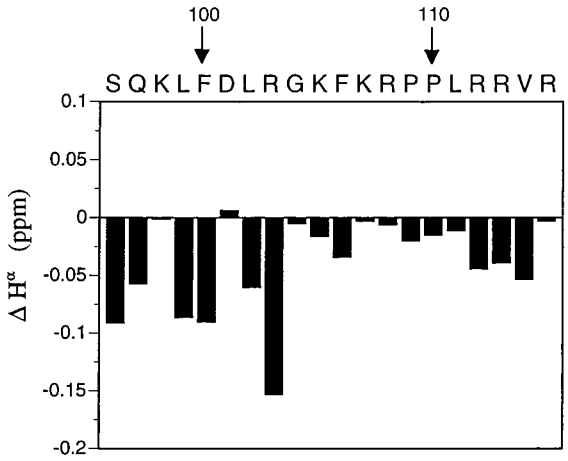

FIGURE 5: Chemical shift differences (ΔH^{α}) for bound minus free H^{α} peptide resonances. The inhibitory peptide sequence is shown in the one-letter amino acid code with the indicated sequence numbering.

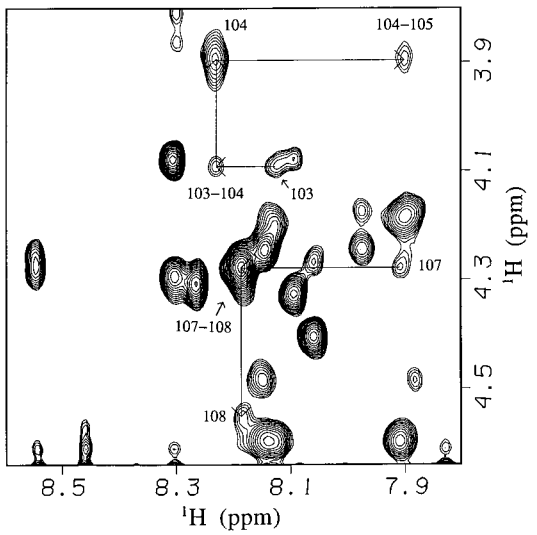

FIGURE 6: H^N-H^{α} region of the ^1H NMR NOESY spectra of TnC-bound TnI(96−115) highlighting intra- to interresidue cross-peaks for segments Arg^{103}-Gly^{104}-Lys^{105} and Lys^{107}-Arg^{108}.

contrast, extended conformations exhibit no nonsequential medium-range NOE connectivities (*31*). No medium-range (i,i+3) or (i,i+4) NOE connectivities are observed for free TnI(96−115) in aqueous solution. A medium-range $H^{\alpha}-H^N$ (i,i+2) NOE for $Gly^{104}-Phe^{106}$ is observed at a lower contour level (not shown). In summary, the NOE data support an extended conformation for the free peptide, possibly bent at Gly^{104}. Free TnI(96−115) in the TFE mixtures shows a chemical shift pattern (data not shown) that differs from the free peptide in aqueous solution as well as from that of the peptide bound to TnC, indicating the TFE-induced structure does not resemble the bound peptide conformation.

NMR Secondary Structure Analysis of TnC-Bound TnI(96−115). $4Ca^{2+}$·dTnC·TnI(96−115) resonance assignments, obtained using standard procedures (*31*), are denoted in the TOCSY spectrum in Figure 4B. H^N-H^{α} cross-peaks for the TnI(96−115) peptide bound to TnC are observed for all residues (except the prolines) with Ser^{96} and Arg^{115} strongly overlapping. Since the TnC component is deuterated, the cross-peaks observed in the $4Ca^{2+}$·dTnC·TnI(96−115) spectra arise only from the TnI(96−115) peptide connectivities.

The differences between the observed chemical shift values for each amino acid and those expected for that amino acid in a random coil can be used as indicators of secondary structure in polypeptides. A grouping of four or more consecutive H^{α} resonances with an upfield chemical shift difference of >0.1 ppm is commonly considered an indicator of a helical segment (*33*). Because the free TnI(96−115) peptide has little or no defined secondary structure based on the CD and NMR results, the H^{α} chemical shift analysis was based on the H^{α} frequency shift differences between the bound and free peptide. This internal calibration circumvents sequence-dependent chemical shift effects which are not always satisfactorily accounted for in model random coil peptide studies. The H^{α} chemical shift differences for the bound peptide minus the free peptide are plotted in Figure 5. Most notably, residues 104−115 exhibit very small (<0.05 ppm) chemical shift differences. This sequence segment corresponds to the peptide sequence previously proposed to form a helix upon binding to TnC on the basis of transferred NOE studies (*15*). The segment of residues 96−104 shows moderately larger H^{α} chemical shifts upon binding, though only one H^{α} chemical shift difference is greater than 0.1 ppm (Arg^{103}). In this segment, Ser^{96}, Leu^{99}, and Phe^{100} exhibit chemical shift differences of ∼0.1 ppm. However, the absence of such shifts for the intervening residues argues against a regular helical structure.

Average intraresidue H^N-H^{α} distances are ∼2.7 Å for both β-sheets and α-helices. In contrast, the sequential $H^{\alpha}-H^N$ average distances are ∼2.2 and ∼3.5 Å for β-sheets and α-helices, respectively. Therefore, if a $1/r^6$-dependent buildup rate is assumed for the cross-peak volumes in the NOESY spectra, the sequential $H^{\alpha}-H^N$ to intraresidue H^N-H^{α} cross-peak volume ratio would be ∼3.4 and ∼0.2 for β-sheets and α-helices, respectively. Figure 4D shows the H^{α} versus H^N region of the ^1H NOESY spectra for the TnC-bound TnI(96−115) where only the sequential connectivities are labeled for clarity (intraresidue connectivities can be deduced from the labeled TOCSY spectra, Figure 4B). The TnC-bound peptide has three sequence segments with distinct volume ratios for all resolved (H^{α} and H^N) cross-peaks: residues 96−102, 103−105, and 106−115. For residues 106−115, the sequential $H^{\alpha}-H^N$ to intraresidue H^N-H^{α} cross-peak volumes are between 3.0 and 5.4, consistent with an extended conformation. As an example, in Figure 6, Lys^{107} and Arg^{108} sequential and intraresidue connectivities are labeled and connected with arrows for the H^{α} versus H^N region of the ^1H NOESY spectra of the TnC-bound TnI(96−115). For residues 96−102, the sequential $H^{\alpha}-H^N$ to intraresidue H^N-H^{α} cross-peak volumes are between 1.4 and 2.8. In this case, the sequential to intraresidue cross-peak volume ratios are smaller than that for a typical β-sheet but at least 7 times larger than the corresponding value for an α-helical structure. In contrast, the short segment consisting of residues 103−105 does not appear to have an extended structure. As is readily apparent in Figure 6, the Gly^{104} intraresidue H^N-H^{α} cross-peak volume is larger than the sequential $H^{\alpha}-H^N$ cross-peak volumes for Arg^{103}-Gly^{104} and Gly^{104}-Lys^{105}, yielding sequential to intraresidue cross-peak volume ratios of 0.24 and 0.45, respectively, suggesting a possible kink in this region. Consistent with the negligible α-helical content

induced in the peptide as a consequence of binding to TnC in the CD studies, NOESY spectra for the dTnC-bound peptide exhibit no medium- or long-range $H^{\alpha}-H^{N}$ NOEs. In summary, the NOE data for TnI(96−115) bound to TnC indicate an extended structure, possibly kinked around Gly^{104}.

In both TnC-bound and free forms of the peptide, only one set of resonances is observed for the proline-rich segment containing residues 108−111 (Arg-Pro-Pro-Leu), indicating there is minimal cis−trans isomerization. Characteristic of trans imides (*31*), $H^{\alpha}-H^{\delta}$ NOE connectivities between residues Arg^{108} and Pro^{109}, $H^{\alpha}-H^{\delta}$ NOE connectivities between Pro^{109} and Pro^{110}, and $H^{\alpha}-H^{N}$ NOE connectivities between Pro^{110} and Leu^{111} were observed for both free and bound peptide. NOE cross-peaks expected for cis imides were not observed. In particular, no $H^{N}-H^{\alpha}$ NOE between residues Arg^{108} and Pro^{109} and no $H^{\delta}-H^{\alpha}$ NOEs between residues Pro^{109} and Pro^{110} or between Pro^{110} and Leu^{111} were observed. Cis imide conformations are either absent or below the noise level, i.e., less than 10% of the population.

DISCUSSION

Our data show that the inhibitory peptide, TnI(96−115), has a predominantly extended conformation upon binding to TnC. Furthermore, the combined CD and NMR data for both the free and TnC-bound peptide are inconsistent with there being any helical structure. The CD data indicate there is only ∼3% helical content in the free peptide in aqueous solution, consistent with results of Cachia and colleagues (*27*) for the shorter TnI(104−115) peptide. Furthermore, the CD spectrum of the peptide complexed with TnC is equal to the sum of the spectra measured for the free components, indicating no net change in helical content upon complex formation. In agreement with the CD results, the NMR data show no evidence for α-helix structure for the TnI(96−115) peptide either free or bound to TnC. The chemical shift differences between free and bound forms show no evidence for the formation of an α-helix as a consequence of binding to TnC. The sequential to intraresidue cross-peak volume ratios support an extended structure for the peptide when bound to TnC with a possible kink at Gly^{104}. While the CD spectrum for the peptide in TFE indicates a propensity for helix formation, albeit at a low level (31% helix in 50% TFE), the NMR data indicate it is a conformation different from either the TnC-bound or free TnI(96−115) in aqueous solution. Therefore, the TFE-induced structure of the free peptide does not mimic the structure induced in the peptide as a consequence of binding to TnC.

On the basis of TRNOE data, Campbell and Sykes (*15*) concluded that the TnI(104−115) peptide forms two helical regions as a consequence of binding to TnC: a helical segment from residue 104 to 108 and a second helix from residue 112 to 115, interrupted by two central proline residues, at positions 109 and 110. They reported medium-range NOE cross-peak connectivities for $H^{\alpha}-H^{N}$ (i,i+3) ($Gly^{104}-Lys^{107}$, $Lys^{105}-Arg^{108}$, and $Arg^{112}-Arg^{115}$) and $H^{\alpha}-H^{N}$ (i,i+4) ($Gly^{104}-Arg^{108}$), none of which was observed for the longer peptide TnI(96−115) (free or bound to TnC) in this study. The experiments described here demonstrate that one can effectively use deuteration to facilitate NMR studies of a peptide in a relatively large complex. This experiment eliminates the ambiguities that can be associated with transferred NOEs due to slow chemical exchange and/or spin diffusion. More recently, Sykes and colleagues have predicted an unstructured segment for residues 104−111 in the TnI(96−148) peptide using their secondary structure prediction algorithm (*34*).

Our CD and NMR results for the bound TnI(96−115) structure are consistent with secondary structure analyses[3] which predict a long helical segment from residues 57−126 interrupted by an unstructured segment starting from residue 102 to 106 and ending between residue 110 and 114 depending on the method used. Two out of five algorithms tested also predict a turn around Gly^{104}. The structure of the TnC-bound peptide may be destabilized at the ends due to the missing neighboring sequence segments in the native TnI. We expect, however, that the central part of the 20-residue peptide will maintain a significant portion of the native TnC−TnI interactions. A number of investigations have recently pointed to an additional important TnC binding site in the sequence segment TnI(115−131) that interacts with the N-terminal domain of TnC (*11*, *35*). However, Pearlstone et al. (*34*) measured the dissociation constants for TnI(96−116) and TnI(96−148) from the C-terminal fragment of TnC and showed only a very modest negative effect due to the loss of TnI(117−148).

The model derived from the neutron contrast variation experiments with the calcium saturated TnC−TnI complex has TnI represented as a superhelical spiral that encompassed TnC and passes through or near the hydrophobic clefts in each globular domain of TnC (*8*). Because there are no high-resolution structural data for TnI, in modeling the neutron data we were constrained to use smooth uniform density geometrical shapes. As a result, the helical spiral shape derived for TnI that best fit the neutron data has a uniform thickness, corresponding to the average thickness of that feature in the structure. This average value is consistent with a predominantly helical secondary structure for the superhelical spiral. The TnI inhibitory peptide (residues 96−115) was predicted to occupy part of the central spiral region of the neutron model. This sequence binds alternately to TnC or to actin in the presence and absence of the Ca^{2+} signal, thus switching the inhibitory function of TnI "off" and "on", respectively. The observed extended structure for the TnI-(96−115) peptide with a kink at Gly^{104} may serve to facilitate a conformational "flip" between its binding sites on TnC and actin during the Ca^{2+}-induced switching process. A uniform helical structure would be less likely to be able to show this type of flexibility. The combined results from our neutron scattering study, secondary structure analyses, CD and NMR data indicate that the helical spiral region of the TnC−TnI model must accomodate the TnI inhibitory segment in an extended−kinked conformation, likely flanked by helical regions on both ends. We suggest that the inhibitory segment could loop out of the superhelical spiral near the N-terminal hydrophobic cleft and the interconnecting helix of TnC, and extend to the C-terminal lobe before it loops back via the kink at Gly^{104} to rejoin the helical spiral path with residues N-terminal to 96. This modification of the neutron-derived model reduces the distance between

[3] SOPMA, available on the World Wide Web at http://www.ibcp.fr/predict.html.

Cys^{48} and Cys^{133} so as to be more consistent with the resonance energy transfer data of Luo et al. (*36*). The helical regions would serve to stabilize the TnC−TnI complex via interactions in the N- and C-terminal lobes of TnC. Ca^{2+} binding to the N-terminal TnC lobe would then modulate its interaction with TnI such that the inhibitory segment can flip between its binding sites on actin or TnC. These studies suggest that models of TnC−TnI interacting in a simple linear anti-parallel configuration may be too simplistic.

ACKNOWLEDGMENT

We thank David LeMaster for many helpful comments on the manuscript, Sue E. Rokop for producing protiated and deuterated TnC, Genevieve Bartlett for technical assistance in the calcium titration of TnC, and Daniel Siath who assisted with purification of the peptide.

REFERENCES

1. Grabarek, Z., Tao, T., and Gergely, J. (1992) *J. Muscle Res. Cell Motil. 13*, 383−393.
2. Herzberg, O., and James, M. N. G. (1985) *Nature 313*, 653−659.
3. Sundaralingam, M., Bergstrom, R., Strasburg, G., Rao, S. T., Roychowdhury, P., Greaser, M., and Wang, B. C. (1985) *Science 227*, 945−948.
4. Potter, J. D., and Gergely, J. (1975) *J. Biol. Chem. 250*, 4628−4633.
5. Herzberg, O., Moult, J., and James, M. N. G. (1986) *J. Biol. Chem. 261*, 2638−2644.
6. Gagné, S. M., Tsuda, S., Li, M. X., Smillie, L. B., and Sykes, B. D. (1995) *Nat. Struct. Biol. 2*, 784−789.
7. Olah, G. A., Rokop, S. E., Wang, C. L. A., Blechner, S. L., and Trewhella, J. (1994) *Biochemistry 33*, 8233−8239.
8. Olah, G. A., and Trewhella, J. (1994) *Biochemistry 33*, 12800−12806.
9. Stone, D. B., Timmins, P. A., Schneider, D. K., Krylova, I., Ramos, C. H. I., Reinach, F. C., and Mendelson, R. A. (1998) *J. Mol. Biol. 281*, 689−704.
10. Vassylyev, D. G., Takeda, S., Wakatsuki, S., Maeda, K., and Maéda, Y. (1998) *Proc. Natl. Acad. Sci. U.S.A. 95*, 4847−4852.
11. Tripet, B., Van Eyk, J. E., and Hodges, R. S. (1997) *J. Mol. Biol. 271*, 728−750.
12. Blechner, S. L., Olah, G. A., Strynadka, N. C. J., Hodges, R. S., and Trewhella, J. (1992) *Biochemistry 31*, 11326−11334.
13. Klevit, R. E., Blumenthal, D. K., Wemmer, D. E., and Krebs, E. G. (1985) *Biochemistry 24*, 8152−8157.
14. Syska, H., Wilkinson, J. M., Grand, R. J. A., and Perry, S. V. (1976) *Biochem. J. 153*, 375−387.
15. Campbell, A. P., and Sykes, B. D. (1991) *J. Mol. Biol. 222*, 405−421.
16. Pearlstone, J. R., and Smillie, L. B. (1995) *Biochemistry 34*, 6932−6940.
17. Seeholzer, S. H., Cohn, M., Putkey, J. A., Means, A. R., and Crespi, H. L. (1986) *Proc. Natl. Acad. Sci. U.S.A. 83*, 3634−3638.
18. London, R. E., Perlman, M. E., and Davis, D. G. (1992) *J. Magn. Reson. 97*, 79−98.
19. Arepalli, S. R., Glaudemans, C. P. J., Daves, G. D., Kovac, P., and Bax, A. (1995) *J. Magn. Reson. B106*, 195−198.
20. Zheng, J., and Post, C. B. (1993) *J. Magn. Reson. B101*, 262−270.
21. Chang, C. T., Wu, C. S. C., and Yang, J. T. (1978) *Anal. Biochem. 91*, 13−31.
22. Slupsky, C. M., Reinach, F. C., Smillie, L. B., and Sykes, B. D. (1995) *Protein Sci. 4*, 1279−1290.
23. Tsuda, S., Hasegawa, Y., Yoshida, M., Yagi, K., and Hikichi, K. (1988) *Biochemistry 27*, 4120−4126.
24. Piotto, M., Saudek, V., and Sklenar, V. (1992) *J. Biomol. NMR 2*, 661−665.
25. Lippens, G., Dhalluin, C., and Wieruszeski, J.-M. (1995) *J. Biomol. NMR 5*, 327−331.
26. Nelson, J. W., and Kallenbach, N. R. (1989) *Biochemistry 28*, 5256−5261.
27. Cachia, P. J., Van Eyk, J., Ingraham, R. H., McCubbin, W. D., Kay, C. M., and Hodges, R. S. (1986) *Biochemistry 25*, 3553−3562.
28. Steiner, R. F., and Norris, L. (1987) *Arch. Biochem. Biophys. 254*, 342−352.
29. Ikura, M., Clore, G. M., Gronenborn, A. M., Zhu, G., Klee, C. B., and Bax, A. (1992) *Science 256*, 632−638.
30. Deslauriers, R., and Smith, I. C. P. (1980) in *Biological Magnetic Resonance* (Berliner, L., and Reuben, J., Eds.) pp 243−344, Plenum Press, New York.
31. Wüthrich, K. (1986) in *NMR of Proteins and Nucleic Acids*, John Wiley and Sons, New York.
32. Neuhaus, D., Wagner, G., Vasák, M., Kägi, J. H. R., and Wüthrich, K. (1995) *Eur. J. Biochem. 151*, 257−273.
33. Wishart, D. S., Sykes, B. D., and Richards, F. M. (1992) *Biochemistry 31*, 1647−1651.
34. Pearlstone, J. R., Sykes, B. D., and Smillie, L. B. (1997) *Biochemistry 36*, 7601−7606.
35. McKay, R. T., Tripet, B. P., Hodges, R. S., and Sykes, B. D. (1997) *J. Biol. Chem. 272*, 28494−28500.
36. Luo, Y., Wu, J.-L., Gergely, J., and Tao, T. (1997) *Biochemistry 36*, 11027−11035.

BI990150Q